Mazars' damage model for masonry structures: a case study of a church in Italy

A. De Falco[1], M. Mori[*1], G. Sevieri[2] [1] Dept. of Energy, Systems, Territory and Construction Engineering, Pisa Univ. (Italy), [2] Dept. of Civil and Environmental Engineering, Florence Univ. (Italy).
*Corresponding Author: largo L. Lazzarino, 1 - 56126 Pisa, morimatteo123@gmail.com

Abstract: Seismic assessments and structural analyses of buildings that are part of the cultural heritage plays an important role in safeguarding their integrity and conservation.
In this paper a Mazars' damage model is used in the characterization of the global dynamic behavior of masonry structures. The model is applied to a medieval church located in Lunigiana (central Italy) which suffered the earthquake in June 2013. The FE analysis demonstrates the importance of taking into account the effect of existing damage in the evaluation of the dynamic behavior of masonry structures.

***Keywords**: FE modeling, historical buildings, modal analysis, Mazars' damage model.*

1. Introduction

Old masonry buildings are particularly vulnerable to seismic actions, due to the very low tensile strength of the material and the intrinsic inhomogeneity. Modern modeling techniques may help in understanding the complex dynamic behavior of such buildings in order to prevent, or at least mitigate, the consequences of an earthquake.
Masonry modeling is challenging due to the lack of knowledge on the internal morphology of the walls, the nonlinear properties of the materials and the great variety of building techniques, which make it difficult to identify the overall mechanical characteristics. The main feature of masonry materials is the strong nonlinear behavior with low-to-negligible tensile strength, which may produce cracking even in the presence of the self-weight only. In addition, during an earthquake, several parts of the structure may suffer tensile loading with subsequent cracking. In turn, the crack pattern can affect the stress distribution, the overall stiffness of the structural elements and the dynamic behavior of the entire construction. For this reason, damage should be taken into account in the analyses in order to prevent erroneous predictions of the seismic response of the structure. Given that the modal analysis is carried out under the hypothesis of linear elasticity, it may be unsuitable for masonry materials, as demonstrated in this paper.
There are many strategies for modeling masonry structures, which vary both in terms of the approach and computational requirements. In this paper, finite element discretization of the continuum was chosen, mainly because of the high degree of accuracy provided by the geometric modeling, together with the fact that the effect of damage on the global dynamic behavior of masonry structures can be simulated.
The cracking of materials can involve various approaches that are classified into two macro-categories: the first has a geometrical approach, which considers a crack as a geometrical entity; the second has a non-geometrical approach, which only updates the constitutive relationship during the propagation of cracks, the mesh remaining unchanged [1]. This latter regards the continuum models and includes smeared cracks and damage mechanics. Within this macro-category, two groups may be identified, the constitutive methods and the kinematic ones. Among the constitutive methods, the continuum damage model (CDM) [2] enables areas to be modelled where damage causes a multitude of micro-cracks that are not necessarily localized.
This paper proposes an application within a continuum damage framework to simulate the structural behavior of a church in Tuscany. The aim of the analysis was to simulate the effects of crack development through a nonlinear constitutive equation of the material with bounded tensile strength. A Mazars' damage model was adopted [3] and the dynamic properties of the construction were also explored after there had been structural damage.
First, the constitutive damage model was validated on a masonry arch subjected to increasing loads, then, an entire church was studied. The modal analysis on the 3D FE model of the church was performed in COMSOL [4], both under the hypothesis of linear elasticity and simulating the damaging material. The effect of damage was thus well highlighted.

2. Mazars' damage model

Mazars' model for concrete is a continuum damage model, where the history of irreversible strains in the material is described by means of internal variables that keep track of their evolution. In particular, the isotropic Mazars' damage formulation introduces a damage variable d which modifies the actual value of Young's modulus

$$E^d = (1-d) \cdot E_0, \qquad (1)$$

where E_0 is the undamaged Young modulus. The total damage d is defined as

$$d = \alpha_t d_t + \alpha_c d_c \qquad (2)$$

where d_t and d_c are the tensile and compressive part of damaged areas, and α_t and α_c are weighting coefficients, defined as functions of the principal values of positive strains ε_t and negative strains ε_c

$$\varepsilon_{ij}^t = (1-d)C_{ijkl}^{-1}\sigma_{kl}^t \quad and \quad \varepsilon_{ij}^c = (1-d)C_{ijkl}^{-1}\sigma_{kl}^c \ (3)$$

C_{ijkl}^{-1} are the components of the compliance tensor. The weighting coefficients are defined as

$$\alpha_t = \sum_{i=1}^3 \left(\frac{\langle\varepsilon_i^t\rangle\langle\varepsilon_i\rangle}{\tilde{\varepsilon}^2}\right)^\beta \quad \text{and} \quad \alpha_c = \sum_{i=1}^3 \left(\frac{\langle\varepsilon_i^c\rangle\langle\varepsilon_i\rangle}{\tilde{\varepsilon}^2}\right)^\beta \quad (4)$$

where the Macaulay brackets indicate replacing negative strains with zeros. An equivalent strain is defined as

$$\tilde{\varepsilon} = \sqrt{\sum_{i=1}^3 (\langle\varepsilon_i\rangle_+)^2} \qquad (5)$$

In the cases of simple uniaxial tension and compression, their value is equal to one and zero respectively. Tensile and compressive damage are then given by

$$d_t(\kappa) = 1 - \frac{\kappa_0(1-A_t)}{\kappa} - A_t e^{-B_t(\kappa-\kappa_0)} \qquad (6)$$

$$d_c(\kappa) = 1 - \frac{\kappa_0(1-A_c)}{\kappa} - A_c e^{-B_c(\kappa-\kappa_0)} \qquad (7)$$

where A_t, B_t, A_c, B_c, and κ_0 are material parameters. κ is the state variable which keeps track of the maximum effective strain, given by $\tilde{\varepsilon}$. κ is initialized to the damage threshold κ_0 which can be defined as a function of maximum tensile strength f_t

$$\kappa_0 = \frac{f_t}{E_0} \qquad (8)$$

The plots in Figure 1 highlight that A governs the residual strength beyond the peak value, and B controls the peak strength itself and the slope of the softening branch. Both parameters affect the fracture toughness, which is proportional to the area below the portion of the stress-strain curve beyond the peak.

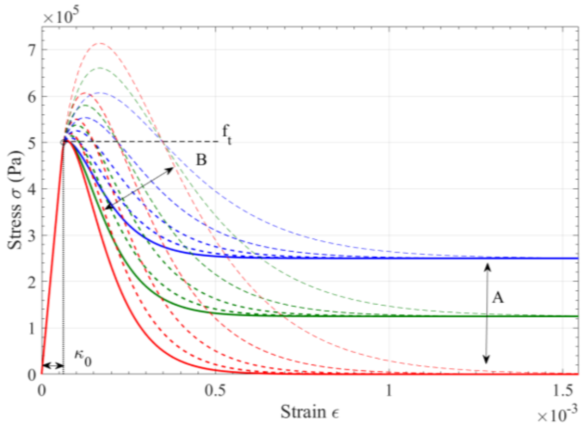

Figure 1. Parameter variation effect on Mazars' model.

3. Basic arch model

A preliminary test was performed on a 2D circular arch, with an 8 m clear span and 1 m thickness, which was loaded at the keystone by a gradually increasing concentrated force applied on a short boundary segment. The plane strain model has unity depth and the mesh is made up of 14226 triangular quadratic serendipity elements and 7418 nodes. Table 1 reports the material parameters, which will also be adopted for the 3D model of the church. In this first model, the results plotted in Figure 2 show the damaged Young modulus beyond ultimate capacity, when the concentrated load attains approximately 300 kN.

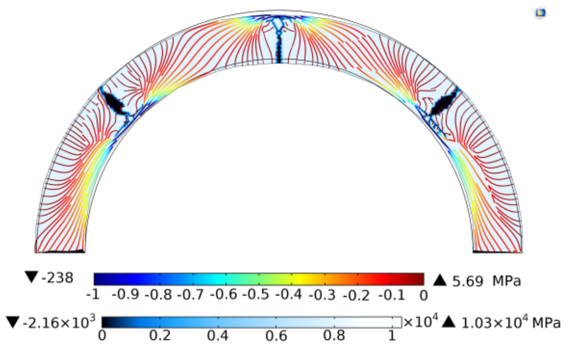

Figure 2. Crack development in the deformed 2D arch model: compression streamlines and damaged elastic modulus.

Note that the damage mechanism follows the usual five-hinge collapse mode in accordance with the literature. The plot also shows the third principal stress streamlines (compression) along with the damaged Young modulus.

Modal analysis was performed both in the undamaged state and after the development of the top hinge. A noticeable drop of the first eigenfrequency from 18.8 to 11.3 Hz was revealed.

4. The case study

The selected case study is San Prospero Church in Monzone Alto in Lunigiana (Tuscany, Italy), located in the upper area of the village, on a rocky outcrop. The church, which dates back to the Middle Ages, was subsequently modified between the 17th and 19th centuries. New baroque and neoclassical architectural elements were added: thick stone masonry vaults and decorative elements such as frames, stuccoes, altars and pilasters. The large rectangular 18th century styled nave of the church houses several valuable altars in polychrome marble which are contained in four circular blind arches into the side walls. The building is covered over by a barrel vault with transverse ribs and lunettes. The triumphal arch opens towards the apsidal basin. Vaulted structures were equipped with chains, presumably included in the construction phase, in order to offset lateral loads. Finally, the bell tower was rebuilt in the twentieth century and is structurally independent from the church.

In 2013 the church suffered an earthquake with a magnitude of ML 5.2, whose epicenter was located around 1 km away. The earthquake did not cause any structural elements to collapse, but only crack patterns appeared on the façade, at the points where façade meets the vaults and at the intrados of the triumphal arch. Figure 3 shows the main cracks.

Figure 3. Crack pattern on the masonry structure of San Prospero church after the 2013 earthquake: on the façade (upper); on the intrados of the triumphal arch (lower).

5. The model of San Prospero church

Defining the correct geometry is fundamental, since the model needs to be an accurate representation of the actual object and should also enable the creation of a manageable mesh in the FE software.

Starting with 2D drawings and site photography, a 3D solid model of the church was created using CAD, as shown in Figure 4. The model was created using a solid extrusion of 2D floor drawings and by lofting 2D sections of the arches and vaults.

The misaligned walls were regularized and the vaulted geometry was simplified in order to achieve a working 3D model in COMSOL. COMSOL's geometric preprocessor was thus used for this purpose, with the help of virtual and Boolean operations to let the software ignore small features.

The final geometry was meshed with the aid of the sizing functionality, by refining the mesh in the vaulted top section, having a maximum size of 25 centimeters, a maximum element growth rate of 1.1 and a curvature factor of 0.25.

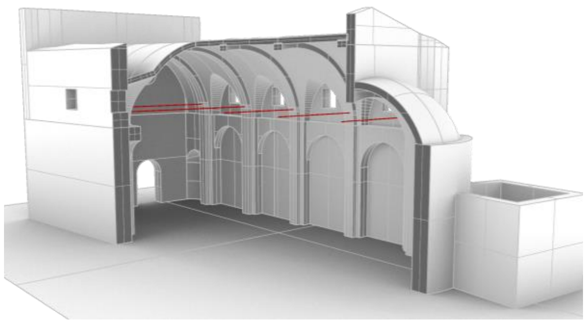

Figure 4. Render of a quarter section view of the 3D CAD model. Tie rods are highlighted in red.

The mesh was composed of 452.439 tetrahedral elements with 3.596.871 degrees of freedom (Figures 5 and 6). *Solid Mechanics* physics was applied and a fixed boundary condition was imposed at the base nodes of the model. Tie rods were introduced using *Shell* physics to capture the nonlinear geometric effects. Since the steel rods had a 3 cm square section, the corresponding surface geometry had a width of 3 cm and a shell thickness of 3 cm.

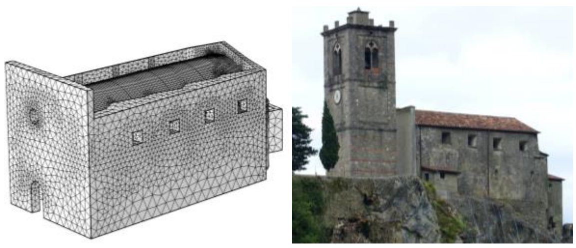

Figure 5. 3D mesh (left) and site exterior view (right).

Shell and solid interfaces were automatically coupled by the Solid-Shell connection multiphysics feature. Tie rods were anchored at the external wall face using steel plates. This detail was reproduced by defining a linear elastic steel solid zone around the anchoring point, coupling the edges to allow for a realistic stress diffusion from the tie to the masonry.

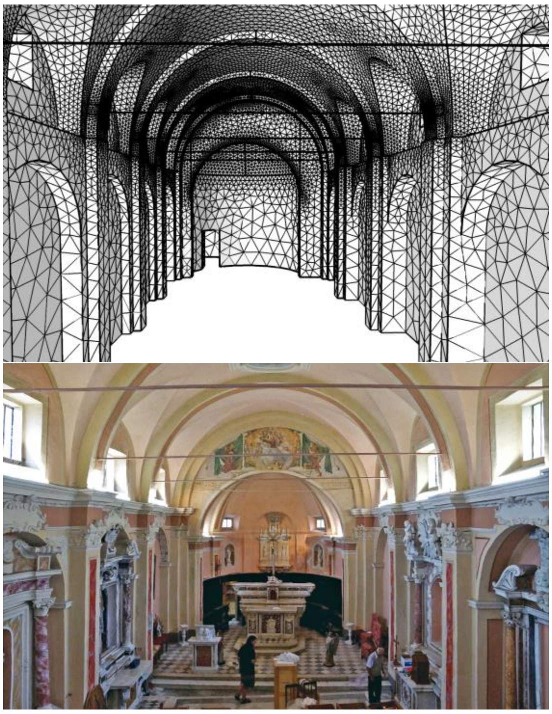

Figure 6. Interior view of 3D model mesh (upper) and site photography (lower).

Mazars' damage model was implemented through COMSOL's external material functionality. This enables the external Dynamic Link Library (DLL) to be referenced, available in COMSOL's application library, which contains Mazars' formulation.

The function requires Mazars' and elasticity parameters in input, along with the current Green-Lagrange strain tensor at each point of the mesh. It then applies the material constitutive model and returns the corresponding second Piola-Kirckhhoff stress tensor. The DLL function is called at each iteration step, until convergence is achieved. If an external material is used, the nonlinear geometry checkbox is automatically enabled, since the stiffness (Jacobian) matrix needs to be updated at each step. Gravity is introduced as a volume load throughout the whole model and its value is gradually ramped with the aid of COMSOL auxiliary sweep functionality, in steps of 10%. The reason for this is that the strong material nonlinearity and softening behavior requires the stiffness matrix to be recomputed in fine steps while solving the model response to the full load history. Solver settings were also modified from default values, using a segregated solver and requiring the Jacobian matrix to be updated at each step.

Masonry			
		Undamaged Young's modulus E_0 (MPa)	8000
		Poisson ratio ν	0.2
		Density (kg/m^3)	2200
Mazars' parameters			
		κ_0	$6.25 \cdot 10^{-6}$
A_t	*1*	B_t	$1 \cdot 10^6$
A_c	1	B_c	$1 \cdot 10^3$
Steel			
		Young's modulus E (MPa)	200000
		Poisson ratio ν	0.3

Table 1. *Material model parameters.*

6. Results for the static analysis

The damaged zones are shown in Figures 7 and 8 where the equivalent damaged Young's modulus distribution is plotted. The figures show that the majority of damage occurs at the intrados of the keystone of the arches, at the connection between the vaults and the masonry walls, and on the upper part of the walls themselves.

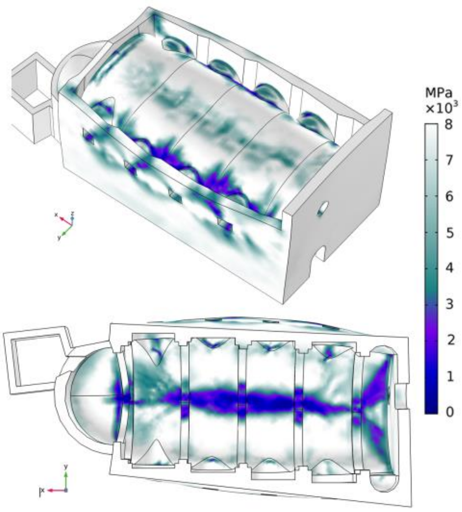

Figure 7. Damaged Young's modulus under the self-weight for the model without tie rods.

The difference between the case with and without tie rods is not striking, however the damaged area at the central intrados of the vault and at the base of the side vaults is less extended in the tied case. The forces in the

ties range from 6 kN for the lateral rods to 14 kN for the central rod.
A modal analysis was then performed starting with the results of the static analysis. The tangent stiffness matrix was thus defined through the damaged Young's modulus E_d, calculated during the static analysis. This was carried out using the previous results as the modal solver linearization point, similarly to a prestressed analysis.

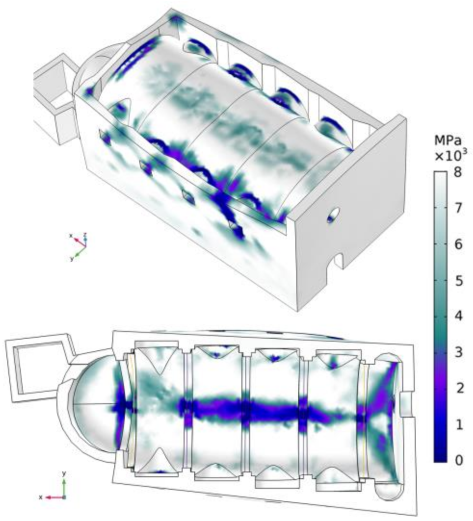

Figure 8. Damaged Young's modulus under the self-weight for the model equipped with tie rods.

The resulting eigenfrequency values from the tied and untied cases were compared with those obtained from the linear elastic model in Table 2. Eigenvectors were normalised such that the modal masses become unity. Figure 9 compares the first three modes showing the displacement magnitude. The damage of the structure noticeably reduces the structural stiffness, thus leading to a decrease in natural vibration frequency. The tie rods mitigate the damage effects but do not restore the total integrity of the structure.

Elastic	Mazars damage model	Mazars damage model + tie rods
10.5	8.8	9.6
14.5	10.3	12.1
19. 0	16.1	17.3
21.5	18.1	19.8
24.0	18.9	20.4
25.8	19.5	21.9

Table 2. First six eigenfrequencies for the three cases (Hz).

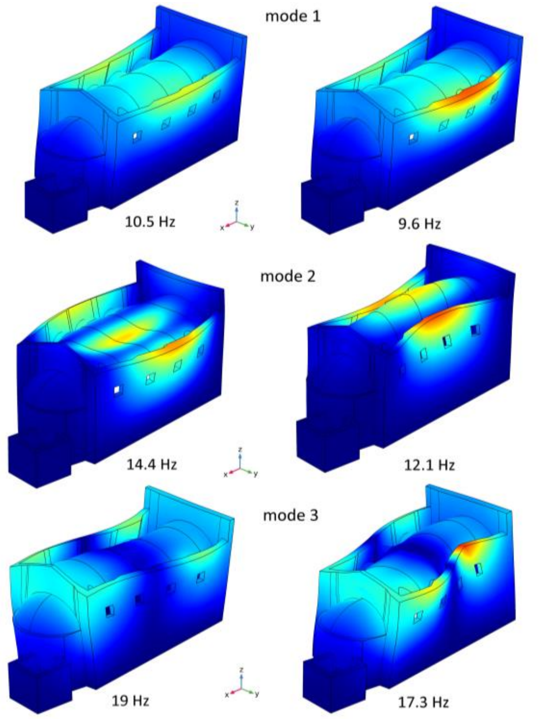

Figure 9. The first three modes shapes for the model of the church equipped with tie rods under the self-weight: linear elastic case (left); Mazars' material (right).

7. Results for the transient analysis

The model was then subjected to a three-axial base acceleration recorded on 21 June 2013 (main shock at UTC 10:33). The recording station, belonging to the national accelerometric network (RAN) [6] with code FVZ, is the closest one to the church. It is located near Fivizzano on E category soil (Eurocode 8 [7]), about 10 km from the epicenter. Figure 10 shows the three acceleration components.

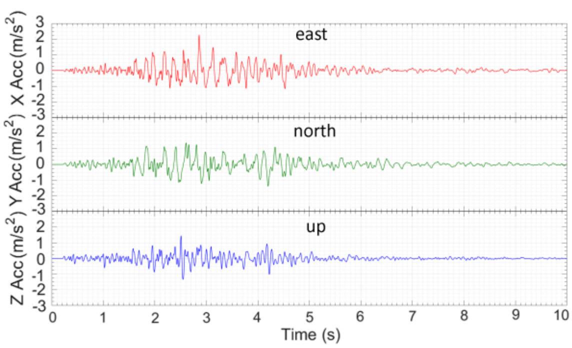

Figure 10. The three acceleration components recorded by station FVZ (10 km from the epicenter).

Figure 11 shows the map of the damaged zone in the form of the damaged equivalent Young's modulus for two different time instants of the transient analysis. The figures highlight that the damage originates in the vaulted structures, in particular at the connection between the façade and the ceiling and near the triumphal arch, as shown by the crack pattern. At the end of the shaking, the damage extends all over the vaults, affecting the side walls only at the top.

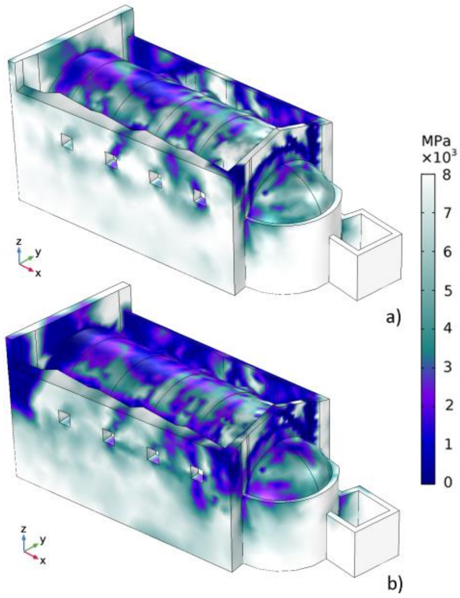

Figure 11. Damaged equivalent Young's modulus for two different time instants of the time history.

The vibration modes were evaluated at the end of the time history. Figure 12 compares the first three vibration modes of the nonlinear model under the self-weight, before and after the shaking.

Figure 13 shows the frequency values for the first six vibration modes of the model in the four cases of linear elasticity, Mazars' material with and without tie rods and after the shaking.

Besides a frequency shift to lower values due to additional damage, the structure after the shock also displays a different second mode shape, compared to the gravity loaded case. It is therefore clear that for masonry structures, the evaluation of the frequency values under the hypothesis of linear elasticity is unacceptable.

Figure 14 reports the map of maximum principal stress under the self-weight and during the time history, showing the different tensile stress distributions in the damaged areas.

Figure 15 shows the compression streamlines in the vaults in the two cases previously analyzed. The figures highlight how the damaged portion remains unloaded upon deformation reversal.

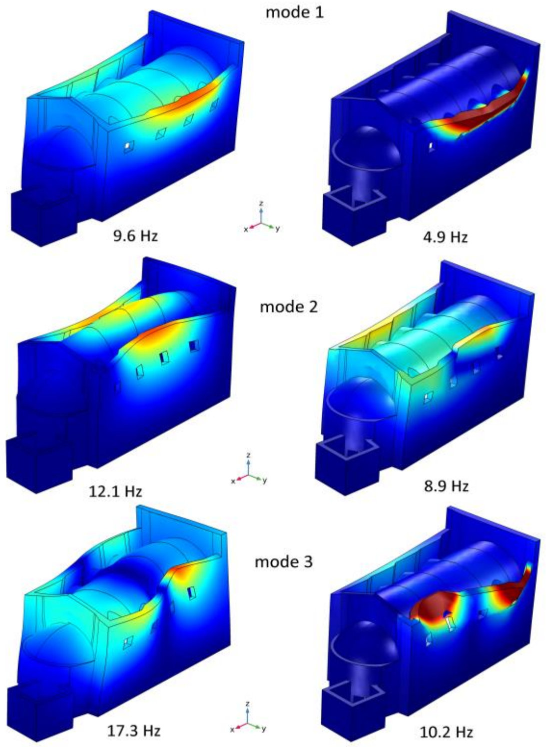

Figure 12. The first three modes shapes for Mazars' model of the church equipped with tie rods under the self-weight, before (left) and after the shaking (right).

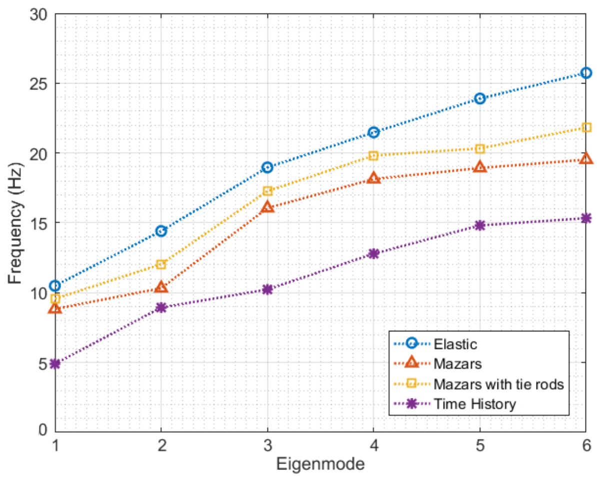

Figure 13. Vibration frequencies for the first six modes in the case of linear elasticity (blue line), Mazars' model without tie rods (red line), Mazars' model with tie rods (yellow line) and Mazars' model with tie rods after the shaking (purple line).

This demonstrates that the hypothesis of Mazars' material captures the damaged areas for monotonic increasing loads, but fails with cyclic loads, thus underestimating the load-carrying capacity of the material at the closing of the cracks.

This problem could affect the simulation accuracy of the dynamic behavior of the construction. Additional hypotheses are therefore possible, such as those already included in the μ-model formulated by Mazars. the μ-model considers the three-axiality of the stress state, introducing two state variables, instead of one. The second state variable enables equivalent damage upon crack closure to be eliminated in the model.

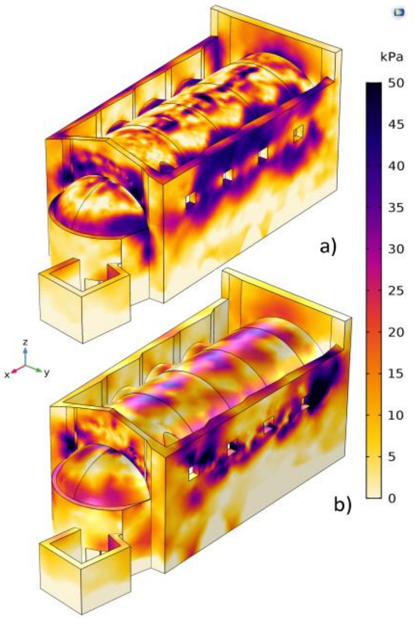

Figure 14. Map of the maximum principal stress under the self-weight, before a) and after b) the seismic shaking.

8. Conclusions

In this work, a masonry structure was modeled using the equivalent continuous model and the constitutive law of Mazars' damaging material. COMSOL enables custom material models to be used in the form of dynamic link libraries. In this case Mazars' model is already available in COMSOL's application library. This study evaluated the change in the dynamic behavior of a masonry structure in relation to the damage level of the material.

It can be concluded that Mazars' hypothesis successfully captures the effects of the damaged areas on the structural behaviour with monotonous loads, however it fails for cyclic loads. To overcome this problem, the external material library could be suitably modified, adding the hypothesis of the μ-model, which was formulated by Mazars [7].

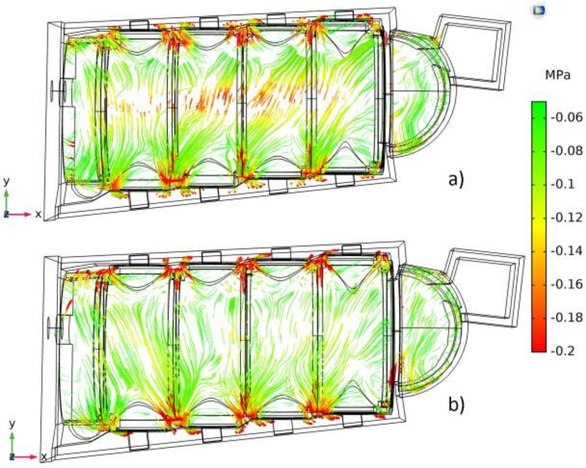

Figure 15. Compression streamlines under the self-weight, before a) and after b) the seismic shaking.

References

1. A.R. Ingraffea, Computational fracture mechanics, in Encyclopedia of Computational Mechanics, John Wiley and Sons, Ltd. (2004).

2. D. Kondo, H. Welemane, F. Cormery. Basic concepts and models in continuum damage mechanics, *Revue Européenne de Génie Civil*, **11**(7-8), 927-943 (2007).

3. J. Mazars, G. Pijaudier-Cabot, Continuum damage theory - application to concrete, *J. of Eng. Mech.*, ASCE, **115**(2), 345–365 (1989).

4. COMSOL Multiphysics®, User's Guide, Version 5.3a (2017).

5. Working Group ITACA (2009) - Data Base of the Italian strong motion data: http://itaca.mi.ingv.it.

6. EN 1998-1: Eurocode 8: Design of structures for earthquake resistance – Part 1: General rules, seismic actions and rules for buildings. (2004)

7. J. Mazars, and F. Hamon,. A new model to forecast the response of concrete structures under severe loadings: the μ-damage model, *Proceedings of VIII International Conference on Fracture Mechanics of Concrete and Concrete Structures FraMCoS-8*, Toledo (Spain), J.G.M. Van Mier, G. Ruiz, C. Andrade, R.C. Yu and X.X. Zhang (Eds) (2013).

Acknowledgements

This research was financially supported by University of Pisa under the research programme "Multi-scale modelling in structural engineering" within "Progetti di Ricerca di Ateneo 2018" (PRA 2018).